

# Coherent effects in magneto-transport through Zeeman split levels

S. A. Gurvitz<sup>1,2</sup>, D. Mozyrsky<sup>2</sup>, and G. P. Berman<sup>2</sup>

<sup>1</sup>Department of Particle Physics, Weizmann Institute of Science, Rehovot 76100, Israel

<sup>2</sup>Theoretical Division and CNLS, Los Alamos National Laboratory, Los Alamos, NM  
87545, USA

(May 24, 2019)

## Abstract

We study non-equilibrium electronic transport through a quantum dot or impurity weakly coupled to ferromagnetic leads. Based on the rate equation formalism we derive noise spectra for the transport current. We show that due to quantum interference between different spin components of the current the spectrum develops a peak or a dip at the frequency corresponding to Zeeman splitting in the quantum dot. The detailed analysis of the spectral structure of the current is carried out for noninteracting electrons as well as in the regime of Coulomb blockade.

## I. INTRODUCTION

Resonant transport through a quantum dot (or impurity) has been investigated in numerous publications. Yet no special attention has been paid to quantum interference effects in this process. These effects can generate oscillations in the resonant current through two (or more) levels of an impurity, similar to the well-known quantum interference effects in the two-slit experiment. These oscillations, in turn would produce a peak or a dip in the current power spectrum, depending on the relative phase of the two levels carrying the current [1], which can be experimentally observed in time-resolved measurements of transport currents [2,3]. It has been previously argued that the quantum interference effect can explain modulation in the tunneling current at the Larmor frequency in scanning tunneling microscope (STM) experiments [4].

In this paper we investigate the interference effects in polarized magneto-transport. Conductance and I-V curves for spin dependent transport through quantum dots has recently been studied in several publications [5–7]. Here we concentrate on the study time dependent properties of transport currents. In particular we study effects related to interference between different spin components of the currents.

These effects can be described schematically as follows. Consider the polarized resonant current from the left reservoir (emitter) to the right reservoir (collector) through a single level of a quantum dot (impurity) in the presence of an external magnetic field. This field would split the resonant level of the dot into the Zeeman doublet, Fig. 1. Let us assume that the polarization axis of electrons in the emitter ( $\mathbf{n}$ ) is different from that of the external magnetic field ( $\bar{\mathbf{n}}$ ). Then a spin-polarized electron from the emitter can enter into either "spin-up" or "spin-down" level of the Zeeman doublet, Fig. 1, or speaking "quantum mechanically", into a superposition of the two spin states. As a result, the electron wave function in the collector would have two components corresponding to different energies of the doublet. Yet these components are orthogonal, since they correspond to different spin components, and therefore cannot interfere. If, however, there is an additional spin-flip process in a transition

between the dot and the collector, the two spin components can interfere in the collector current. Again, this takes place if polarization in the collector ( $\mathbf{n}'$ ) is different from that in the quantum dot ( $\bar{\mathbf{n}}$ ), Fig. 1.

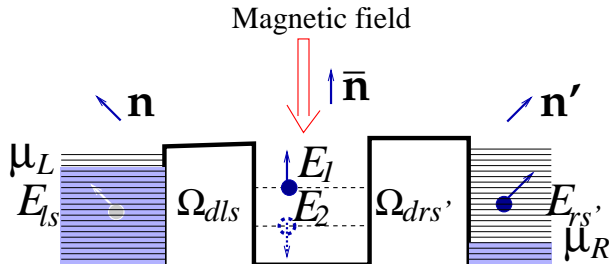


Fig. 1. Resonant tunneling of a polarized electron through a quantum dot. Here  $\Omega$ 's denote the tunneling transition amplitudes between the reservoir states and the Zeeman doublets ( $E_{1,2}$ ) of the quantum dot.  $\mu_{L,R}$  are the chemical potential in the left and right reservoirs. The unit vectors  $\mathbf{n}$ ,  $\bar{\mathbf{n}}$  and  $\mathbf{n}'$  show polarization axes in the emitter, quantum dot, and the collector, respectively.

The described interference effects can be realized experimentally in a heterostructure with a quantum dot sandwiched between the two ferromagnetic leads with easy axes different from those in the dot. Similar magnetic multilayer systems are likely to find prominent technological applications, such as random access memory, magnetic sensors, etc., due to the giant magnetoresistance effect [8]. An external magnetic field is needed to control the value of Zeeman splitting in the dot, e.g. Fig. 1.

The plan of this paper is as follows. In Sect. II we consider polarized resonant transport through a Zeeman doublet in the framework of noninteracting electrons. We elaborate the mechanism of quantum oscillations in the resonant current and necessary conditions for their observation. In particular, we demonstrate that the oscillations disappear in the unpolarized current. In Sect. III we consider the many-electron case. For the evaluation of resonant current we use the rate equations approach obtained directly from the many-

body Schrödinger equation describing the entire system [9,10]. We compare this approach with single-electron model in the case of non-interacting electrons. Also in this section we consider the system with ferromagnetic leads and show that for such case the total current exhibits oscillations due to interference effects. In Sect. IV we concentrate on the interacting case. In particular we derive current spectra in the presence of Coulomb blockade in the dot. In Sect. V we summarize our calculations and briefly discuss potential implications of our results on noise spectroscopy of quantum dots.

## II. INDEPENDENT PARTICLE MODEL

Consider polarized transport of non-interacting electrons through a quantum dot in the external magnetic field, Fig. 1. The polarization axis of an electron inside the dot ( $\bar{\mathbf{n}}$ ) is different from those in the right and left reservoirs ( $\mathbf{n}$  and  $\mathbf{n}'$ ). The tunneling Hamiltonian describing this system can be written as

$$H = \sum_{l,s} E_{ls} a_{ls}^\dagger a_{ls} + \sum_{d=1,2} E_d a_d^\dagger a_d + \sum_{r,s'} E_{rs'} a_{rs'}^\dagger a_{rs'} + \left( \sum_{d,l,s} \Omega_{dls} a_{ls}^\dagger a_d + \sum_{d,r,s'} \Omega_{drs'} a_{rs'}^\dagger a_d + H.c \right), \quad (1)$$

where the spin indices,  $s, s' = \pm 1/2$  are related to different quantization axes ( $\mathbf{n}$  and  $\mathbf{n}'$ , Fig. 1), and  $E_{ls}, E_{rs'}$  denote the energy levels in the reservoirs. The Zeeman split energy of the dot is denoted by  $E_d$ , where  $d = 1, 2$ . The last terms describes tunneling transitions between the reservoirs and the dot states generated by the tunneling couplings  $\Omega$ .

All parameters of the tunneling Hamiltonian (1) are related to the initial microscopic description of the system in the configuration space ( $\mathbf{x}$ ). For instance, the coupling  $\Omega_{dls}$  is given by the Bardeen formula [11]

$$\Omega_{dls} = -\frac{1}{2m} \int_{\mathbf{x} \in \Sigma_l} \phi_d(\mathbf{x}) \overleftrightarrow{\nabla} \chi_{ls}(\mathbf{x}) d\sigma, \quad (2)$$

where  $\phi_d(\mathbf{x})$  and  $\chi_{ls}(\mathbf{x})$  are the electron wave functions inside the dot and the reservoir, respectively and  $\Sigma_l$  is a surface inside the potential barrier that separates the dot from the

left reservoir. Since spin quantization axes in the dot and in the leads differ from each other, the transition matrix elements ( $\Omega$ 's) in Eq. (2) depend on the relative angles between the dot and the leads polarization axes ( $\theta_L$  and  $\theta_R$  for left and right leads respectively). The simplest form of the matrix elements that respects SU(2) symmetry corresponds to

$$\Omega_{dls} = \Omega_l \mathbf{d}_{s,s_d}^{(1/2)}(\theta_L) \quad \text{and} \quad \Omega_{drs'} = \Omega_r \mathbf{d}_{s_d,s'}^{(1/2)}(\theta_R), \quad (3)$$

where  $s_d = \pm 1/2$  denotes the electron spin inside the dot, Fig. 1,  $\Omega_{l/r}$  is spin-independent part of the matrix element, and  $\mathbf{d}^{(1/2)}(\theta)$  is spin rotation matrix,

$$\mathbf{d}^{1/2}(\theta) = \begin{pmatrix} \cos \frac{\theta}{2} & \sin \frac{\theta}{2} \\ -\sin \frac{\theta}{2} & \cos \frac{\theta}{2} \end{pmatrix}. \quad (4)$$

Non-interacting electron transport through a quantum dot can be described in terms of a single-electron time-dependent wave function [12]. The latter can be written in the most general way as

$$|\Psi(t)\rangle = \left[ \sum_{l,s} \mathbf{b}_{ls}(t) a_{ls}^\dagger + \sum_{d=1,2} \mathbf{b}_d(t) a_d^\dagger + \sum_{r,s'} \mathbf{b}_{rs'}(t) a_{rs'}^\dagger \right] |0\rangle, \quad (5)$$

where  $\mathbf{b}_\alpha(t)$  is the amplitude of finding the electron in the state  $\alpha$  given by a corresponding creation operator. Substituting  $|\Psi(t)\rangle$  in the Schrödinger equation  $i\partial_t|\Psi(t)\rangle = H|\Psi(t)\rangle$  we obtain the following system of the linear differential equations, defining the amplitudes  $\mathbf{b}_\alpha(t)$ :

$$i\dot{\mathbf{b}}_{ls}(t) = E_{ls}\mathbf{b}_{ls}(t) + \sum_{d=1,2} \Omega_{dls}\mathbf{b}_d(t) \quad (6a)$$

$$i\dot{\mathbf{b}}_d(t) = E_d\mathbf{b}_d(t) + \sum_{l,s} \Omega_{dls}\mathbf{b}_{ls}(t) + \sum_{r,s'} \Omega_{drs'}\mathbf{b}_{rs'}(t) \quad (6b)$$

$$i\dot{\mathbf{b}}_{rs'}(t) = E_{rs'}\mathbf{b}_{rs'}(t) + \sum_{d=1,2} \Omega_{drs'}\mathbf{b}_d(t) \quad (6c)$$

Let us assume that the electron is initially in the left reservoir (emitter) at the level  $E_l$  with the spin polarized along the  $\mathbf{n}$ -direction, Fig. 1. This corresponds to the initial conditions  $\mathbf{b}_{ls}(0) = \delta_{l,\bar{l}}\delta_{s,1/2}$  and  $\mathbf{b}_d(0) = \mathbf{b}_{rs}(0) = 0$ . In order to solve Eqs. (6) it is useful to perform the Laplace transform,  $\tilde{\mathbf{b}}(E) = \int_0^\infty \mathbf{b}(t) \exp(iEt)dt$ . As a result Eqs. (6) become

$$(E - E_{ls})\tilde{\mathbf{b}}_{ls}(E) - \Omega_l \sum_{d'=1,2} \mathbf{d}_{s,s_{d'}}^{(1/2)}(\theta_L)\tilde{\mathbf{b}}_{d'}(E) = i\delta_{l,\bar{l}}\delta_{s,1/2} \quad (7a)$$

$$(E - E_d)\tilde{\mathbf{b}}_d(E) - \sum_{l,s} \Omega_l \mathbf{d}_{s_d,s}^{(1/2)}(\theta_L)\tilde{\mathbf{b}}_{ls}(E) - \sum_{r,s'} \Omega_r \mathbf{d}_{s_d,s'}^{(1/2)}(\theta_R)\tilde{\mathbf{b}}_{rs'}(E) = 0 \quad (7b)$$

$$(E - E_{rs'})\tilde{\mathbf{b}}_{rs'}(E) - \Omega_r \sum_{d'=1,2} \mathbf{d}_{s',s_{d'}}^{(1/2)}(\theta_R)\tilde{\mathbf{b}}_{d'}(E) = 0. \quad (7c)$$

Now we substitute  $\tilde{\mathbf{b}}_{ls}$  and  $\tilde{\mathbf{b}}_{rs'}$  from Eqs. (7a), (7c) into Eq. (7b). Neglecting the energy dependence of the couplings,  $\Omega_{l,r} = \Omega_{L,R}$ , and replacing the sums on  $l$  and  $r$  by the integrals, we obtain

$$\left(E - E_1 + i\frac{\Gamma_L + \Gamma_R}{2}\right)\tilde{\mathbf{b}}_1(E) = i\frac{\Omega_L \cos(\theta_L/2)}{E - E_{\bar{l},1/2}} \quad (8a)$$

$$\left(E - E_2 + i\frac{\Gamma_L + \Gamma_R}{2}\right)\tilde{\mathbf{b}}_2(E) = -i\frac{\Omega_L \sin(\theta_L/2)}{E - E_{\bar{l},1/2}} \quad (8b)$$

where  $\Gamma_{L,R} = 2\pi\Omega_{L,R}^2\rho_{L,R}$ , and  $\rho_{L,R}$  is density of the states in the left (right) reservoir. Note that the amplitudes  $\tilde{\mathbf{b}}_1(E)$  and  $\tilde{\mathbf{b}}_2(E)$  are decoupled in Eqs. (8) although the corresponding states are connected via continuum. The reason is that the spin-flip couplings of the dot with the reservoirs are of the opposite sign for the spin-up and the spin-down states of the dot ( $E_1$  and  $E_2$  in Fig. 1). However, in general case of resonant tunneling through two levels, the corresponding amplitudes are coupled via interaction through continuum [1].

Using the inverse Laplace transform  $\mathbf{b}_{1,2}(t) = \int \tilde{\mathbf{b}}_{1,2}(E) \exp(-iEt) dE / (2\pi)$ , we obtain for the amplitudes  $\mathbf{b}_{1,2}(t)$  for finding the electron inside the dot

$$\mathbf{b}_1(t) = \frac{\Omega_L \cos(\theta_L/2)}{E_L - E_1 + i\frac{\Gamma}{2}} \left( e^{-iE_L t} - e^{-iE_1 t - \frac{\Gamma}{2}t} \right) \quad (9a)$$

$$\mathbf{b}_2(t) = -\frac{\Omega_L \sin(\theta_L/2)}{E_L - E_2 + i\frac{\Gamma}{2}} \left( e^{-iE_L t} - e^{-iE_2 t - \frac{\Gamma}{2}t} \right), \quad (9b)$$

where  $\Gamma = \Gamma_L + \Gamma_R$ . Respectively, the probability amplitude of finding the electron inside the collector is  $\tilde{\mathbf{b}}_{rs'}(t) = \int \tilde{\mathbf{b}}_{rs'}(E) \exp(-iEt) dE / (2\pi)$ , where  $\tilde{\mathbf{b}}_{r,s'}(E)$  is given by Eq. (7c)

$$\tilde{\mathbf{b}}_{rs'}(E) = \frac{\Omega_R}{E - E_{rs'}} \sum_d \mathbf{d}_{s',s_d}^{(1/2)}(\theta_R)\tilde{\mathbf{b}}_d(E). \quad (10)$$

The above equations determine the motion of a single electron placed initially in the emitter. In order to obtain the total current in the framework of this model one has to

sum over all initially occupied states  $E_l$  of the emitter and over all available states  $E_r$  of the collector. One finds that the average number of electrons with spin-up and spin-down ( $s' = \pm 1/2$ ), accumulated in the collector by the time  $t$  is  $N_{s'}(t) = \sum_{\bar{l},r} |\mathbf{b}_{rs'}(t)|^2$ . Respectively, the corresponding spin current in the collector,  $I_{s'}$ , is  $dN_{s'}(t)/dt$ . Using the inverse Laplace transform and replacing  $\sum_{\bar{l},r} \rightarrow \int \rho_L \rho_R dE_L dE_R$  we obtain

$$N_{s'}(t) = \int \rho_L \rho_R dE_L dE_R \int \frac{dE dE'}{(2\pi)^2} \tilde{\mathbf{b}}_{rs'}(E) \tilde{\mathbf{b}}_{rs'}^*(E') e^{i(E'-E)t} \quad (11)$$

Consider for the definiteness the polarized current,  $I_{1/2}(t)$ . Substituting Eq. (10) into Eq. (11) and integrating over  $E_{rs'}$  one obtains

$$\begin{aligned} I_{1/2}(t) &= \Gamma_R \int_{\mu_R}^{\mu_L} \rho_L dE_L \int \frac{dE dE'}{(2\pi)^2} e^{i(E'-E)t} [\cos(\theta_R/2) \tilde{\mathbf{b}}_1(E) - \sin(\theta_R/2) \tilde{\mathbf{b}}_2(E)] \\ &\quad \times [\cos(\theta_R/2) \tilde{\mathbf{b}}_1^*(E') - \sin(\theta_R/2) \tilde{\mathbf{b}}_2^*(E')] \\ &= \Gamma_R \int_{\mu_R}^{\mu_L} \rho_L dE_L |\cos(\theta_R/2) \mathbf{b}_1(t) - \sin(\theta_R/2) \mathbf{b}_2(t)|^2, \end{aligned} \quad (12)$$

where the amplitudes  $\mathbf{b}_{1,2}(t)$  are given by Eqs. (9). Note that these amplitudes in the stationary limit,  $\mathbf{b}_{1,2}(t \rightarrow \infty)$ , are the transmission amplitudes describing the resonance tunneling through the levels  $E_{1,2}$ , respectively. Thus Eq. (12) represent a generalization of the Landauer formula for a time-dependent case.

For large bias,  $\mu_L - \mu_R \gg \Gamma$ , the integration over  $E_L$  in Eq. (12) can be performed analytically. Using Eqs. (8) we find

$$\begin{aligned} I_{1/2}(t) &= \Gamma_L \Gamma_R \int \frac{dE dE'}{(2\pi)^2} \left( \frac{\cos(\theta_L/2) \cos(\theta_R/2)}{E - E_1 + i\frac{\Gamma}{2}} + \frac{\sin(\theta_L/2) \sin(\theta_R/2)}{E - E_2 + i\frac{\Gamma}{2}} \right) \\ &\quad \times \left( \frac{\cos(\theta_L/2) \cos(\theta_R/2)}{E' - E_1 - i\frac{\Gamma}{2}} + \frac{\sin(\theta_L/2) \sin(\theta_R/2)}{E' - E_2 - i\frac{\Gamma}{2}} \right) \frac{1}{E' - E} e^{i(E'-E)t} \end{aligned} \quad (13)$$

The last integrations over  $E, E'$  variables can be performed by closing the integration contours to the upper or lower complex  $E, E'$  plane. As a result we finally obtain

$$\begin{aligned} I_{1/2}(t) &= \frac{\Gamma_L \Gamma_R}{2\Gamma} (1 + \cos \theta_L \cos \theta_R) (1 - e^{-\Gamma t}) \\ &\quad + \frac{\Gamma_L \Gamma_R \Gamma \sin \theta_L \sin \theta_R}{2(\epsilon^2 + \Gamma^2)} \left[ 1 - e^{-\Gamma t} \cos(\epsilon t) + e^{-\Gamma t} \frac{\epsilon}{\Gamma} \sin(\epsilon t) \right], \end{aligned} \quad (14)$$

where  $\epsilon = E_1 - E_2$ . This expression clearly displays damped oscillations of the resonant current with frequency  $\epsilon$ . An example of these oscillations in the polarized current is shown in Fig. 2.

The polarized current  $I_{-1/2}(t)$  can be evaluated in the same way. One finds

$$I_{-1/2}(t) = \frac{\Gamma_L \Gamma_R}{2\Gamma} (1 - \cos \theta_L \cos \theta_R) (1 - e^{-\Gamma t}) - \frac{\Gamma_L \Gamma_R \Gamma \sin \theta_L \sin \theta_R}{2(\epsilon^2 + \Gamma^2)} \left[ 1 - e^{-\Gamma t} \cos(\epsilon t) + e^{-\Gamma t} \frac{\epsilon}{\Gamma} \sin(\epsilon t) \right], \quad (15)$$

As a result the total current

$$I(t) = I_{1/2}(t) + I_{-1/2}(t) = \frac{\Gamma_L \Gamma_R}{\Gamma} (1 - e^{-\Gamma t}) \quad (16)$$

does not display any oscillations, Fig. 2, although the electrons are polarized in the initial state.

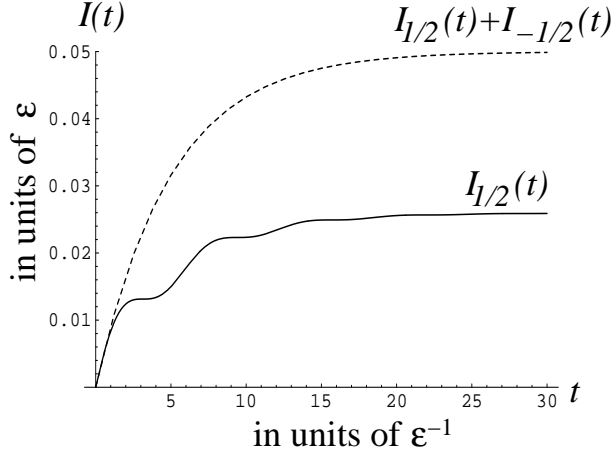


Fig. 2. Polarized and unpolarized resonant current through the Zeeman doublet as a function of time for  $\theta_L = \theta_R = \pi/2$  and  $\Gamma_L = \Gamma_R = 0.1\epsilon$ .

### III. MANY-BODY DESCRIPTION.

Although the single-particle model reproduces quantum interference effects in the magneto-transport, it ignores the electron-electron repulsion inside the dot. The latter



can be taken into account by an additional (interacting) term in the total Hamiltonian,  $\mathcal{H} = H + H_{int}$ , where  $H_{int} = U_C a_1^\dagger a_1 a_2^\dagger a_2$  and  $H_C$  is the Coulomb repulsion energy of two electrons inside the dot.

In the case of large bias,  $|E_{1,2} - \mu_{L,R}| \ll \Gamma_{L,R}$ , the many-body Coulomb repulsion effects in the magneto-transport can be accounted for in the most simple and precise way by using the modified Bloch-type equations for the reduced density matrix [9,10]. These equations can be derived from the many-body Schrödinger equation by integrating out the reservoir states in the limit of weak or strong Coulomb repulsion,  $U_C \ll \mu_L - E_1$  or  $U_C \gg \mu_L - E_1$ , without any stochastic or other approximations. In addition these equations are very useful for evaluation of the shot-noise power spectrum.

In order to apply our method we first redefine the vacuum state,  $|\mathbf{0}\rangle$ , by identifying it with the initial state of the entire system. For instance we can take it corresponding to empty dot, whereas the emitter and collector are filled by up to the chemical potentials  $\mu_{L,R}$ , respectively. In this case the many-body wave function can be written in the most general way as

$$|\Psi(t)\rangle = \left[ b_0(t) + \sum_{d,l,s} b_{dls}(t) a_d^\dagger a_{ls} + \sum_{l,s,r,s'} b_{rs'ls}(t) a_{rs'}^\dagger a_{ls} \right. \\ \left. + \sum_{l,s,\bar{l},\bar{s}} b_{12l\bar{s}\bar{s}}(t) a_1^\dagger a_2^\dagger a_{ls} a_{\bar{l}\bar{s}} + \sum_{d,l,s,\bar{l},\bar{s},r,s'} b_{drs'ls\bar{l}\bar{s}r}(t) a_d^\dagger a_{rs'}^\dagger a_{ls} a_{\bar{l}\bar{s}} + \dots \right] |\mathbf{0}\rangle, \quad (17)$$

where  $d = \{1, 2\}$  denotes a state with one electron in the dot and  $ls(rs')$  denote the electron level in the emitter (collector). The amplitudes  $b_\alpha(t)$  of finding the entire system in the state “ $\alpha$ ” are obtained from the Schrödinger equation,  $i\partial_t |\Psi(t)\rangle = \mathcal{H} |\Psi(t)\rangle$  with the initial condition  $b_\alpha(0) = \delta_{\alpha,0}$

Let us introduce the (reduced) density matrix  $\sigma_{jj'}^{m,n}(t)$ , where  $n, m$  denote the number of electrons arriving the right reservoir with the spin components  $s' = \pm 1/2$ , respectively, Figs. 1,3. The lower indices,  $j, j'$  denote the discrete states of the quantum dot. For instance, in the case of non-interacting (or weakly interacting) electrons  $j, j' = \{0, 1, 2, 3\}$ , Fig. 3. This density matrix,  $\sigma_{jj'}^{m,n}(t)$  can be easily constructed from the amplitudes  $b(t)$ , Eq. (17). For

example,

$$\begin{aligned}\sigma_{00}^{0,0}(t) &= |b_0(t)|^2, & \sigma_{11}^{0,0}(t) &= \sum_l |b_{1l1/2}(t)|^2, & \sigma_{22}^{0,0}(t) &= \sum_l |b_{2l1/2}(t)|^2, & \sigma_{33}^{0,0}(t) &= \sum_{l,\bar{l}} |b_{2l\bar{l}}(t)|^2, \\ \sigma_{12}^{0,0}(t) &= \sum_l b_{1l1/2}(t) \mathbf{b}_{2l1/2}^*(t), & \sigma_{00}^{1,0}(t) &= \sum_{l,r} |b_{1l1/2r1/2}(t)|^2, & \dots\end{aligned}\quad (18)$$

The diagonal density matrix elements,  $\sigma_{jj}^{n,m}$ , are probabilities of finding the system in one of the states shown in Fig. 3, and the off-diagonal matrix elements (“coherencies”), describe the linear superposition of these states.

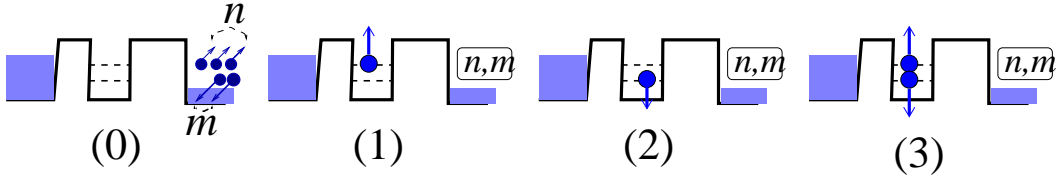


Fig. 3. Four available states of the quantum dot. The indices  $n, m$  denote the number of electrons with the spin components  $s' = \pm 1/2$  in the right reservoir.

It was demonstrated in Ref. [9,10] that the Schrödinger equation for the entire system,  $i\partial_t|\Psi(t)\rangle = \mathcal{H}|\Psi(t)\rangle$ , can be reduced to Bloch-type rate equations describing the reduced density-matrix  $\sigma_{jj'}^{n,m}(t)$ . This reduction takes place after partial tracing over the reservoir states. It becomes the exact one in the limit of large bias without explicit use of any Markov-type or weak coupling approximations [13]. In general case these equations are [10]

$$\begin{aligned}\dot{\sigma}_{jj'} &= i(E_{j'} - E_j)\sigma_{jj'} + i \left( \sum_k \sigma_{jk} \tilde{\Omega}_{k \rightarrow j'} - \sum_k \tilde{\Omega}_{j \rightarrow k} \sigma_{kj'} \right) \\ &- \sum_{k,k'} \mathcal{P}_2 \pi \rho (\sigma_{jk} \Omega_{k \rightarrow k'} \Omega_{k' \rightarrow j'} + \sigma_{kj'} \Omega_{k \rightarrow k'} \Omega_{k' \rightarrow j}) + \sum_{k,k'} \mathcal{P}_2 \pi \rho (\Omega_{k \rightarrow j} \Omega_{k' \rightarrow j'} + \Omega_{k \rightarrow j'} \Omega_{k' \rightarrow j}) \sigma_{kk'},\end{aligned}\quad (19)$$

(for simplicity we have omitted the indices  $m$  and  $n$ , which, however, can be easily restored from the conservation of the total number of electrons). Here  $\Omega_{k \rightarrow k'}$  denotes one-electron

hopping amplitude that generates  $k \rightarrow k'$  transition. We distinguish between the amplitudes  $\tilde{\Omega}$  describing one-electron hopping among isolated states and  $\Omega$  generating transitions among isolated and continuum states. The latter can generate transitions between the isolated states of the system, but only indirectly, via two consecutive hoppings of an electron across the *continuum* reservoir states (with the density of states  $\rho$ ). These transitions are represented by the third and the fourth terms of Eq. (19). The third term describes transitions  $(k \rightarrow k' \rightarrow j)$  or  $(k \rightarrow k' \rightarrow j')$ , which cannot change the number of electrons  $(n, m)$  in the collector. The fourth term describes transitions  $(k \rightarrow j \text{ and } k' \rightarrow j')$  or  $(k \rightarrow j' \text{ and } k' \rightarrow j)$  which increase the number of electrons in the collector by one. These two terms of Eq. (19) are analogues to the “loss” (negative) and the “gain” (positive) terms in the classical rate equations, respectively. Yet, the sign of these terms depends on a relative sign of the corresponding couplings  $\Omega$  [1]. In our case it is the sign of the spin-flip amplitude, Eq. (3). In addition, there is a (permutation) factor,  $\mathcal{P}_2 = \pm 1$ , due to anti-commutation of the fermions operators,  $a_{1,2}^\dagger$  in Eq. (17) (see also [9]). Prefactor  $\mathcal{P}_2 = -1$  whenever the loss or the gain terms in Eq. (19) are generated by the two-particle state of the dot. Otherwise  $\mathcal{P}_2 = 1$ .

We first apply our approach for non-interacting (or weakly interacting) electrons, where the final results for the resonant current should coincide with those obtained in the previous section.

### A. Non-interacting electrons.

Consider first the case of no electron repulsion inside the dot,  $U_C = 0$ . (In fact, the results would be the same for  $U_C \ll \mu_L - E_1$ , assuming the the couplings  $\Omega$  are independent of energy). Similarly to the previous section we choose the initial (“vacuum”) state corresponding to the polarized electrons in the left reservoir,  $s = 1/2$  (Fig. 1). In this case all four configurations shown in Fig. 3 contribute to Eqs. (19). Taking into account that there is no direct coupling between the states,  $E_{1,2}$ , i.e.  $\tilde{\Omega} = 0$ , one obtains the following

Bloch-type rate equations for the density matrix  $\sigma_{jj'}^{n,m}(t)$

$$\begin{aligned}\dot{\sigma}_{00}^{n,m} = & -\Gamma_L \sigma_{00}^{n,m} + \Gamma_R \cos^2 \frac{\theta_R}{2} (\sigma_{11}^{n-1,m} + \sigma_{22}^{n,m-1}) + \Gamma_R \sin^2 \frac{\theta_R}{2} (\sigma_{11}^{n,m-1} + \sigma_{22}^{n-1,m}) \\ & + \Gamma_L \left( \sin^2 \frac{\theta_L}{2} \sigma_{11}^{n,m} + \cos^2 \frac{\theta_L}{2} \sigma_{22}^{n,m} \right) + \frac{\Gamma_L}{2} \sin \theta_L (\sigma_{12}^{n,m} + \sigma_{21}^{n,m}) \\ & - \frac{\Gamma_R}{2} \sin \theta_R (\sigma_{12}^{n-1,m} + \sigma_{21}^{n-1,m} - \sigma_{12}^{n,m-1} - \sigma_{21}^{n,m-1})\end{aligned}\quad (20a)$$

$$\begin{aligned}\dot{\sigma}_{11}^{n,m} = & - \left( \Gamma_R + 2\Gamma_L \sin^2 \frac{\theta_L}{2} \right) \sigma_{11}^{n,m} + \Gamma_L \cos^2 \frac{\theta_L}{2} (\sigma_{00}^{n,m} + \sigma_{33}^{n,m}) - \frac{\Gamma_L}{2} \sin \theta_L (\sigma_{12}^{n,m} + \sigma_{21}^{n,m}) \\ & + \Gamma_R \left( \sin^2 \frac{\theta_R}{2} \sigma_{33}^{n-1,m} + \cos^2 \frac{\theta_R}{2} \sigma_{33}^{n,m-1} \right)\end{aligned}\quad (20b)$$

$$\begin{aligned}\dot{\sigma}_{22}^{n,m} = & - \left( \Gamma_R + 2\Gamma_L \cos^2 \frac{\theta_L}{2} \right) \sigma_{22}^{n,m} + \Gamma_L \sin^2 \frac{\theta_L}{2} (\sigma_{00}^{n,m} + \sigma_{33}^{n,m}) - \frac{\Gamma_L}{2} \sin \theta_L (\sigma_{12}^{n,m} + \sigma_{21}^{n,m}) \\ & + \Gamma_R \left( \cos^2 \frac{\theta_R}{2} \sigma_{33}^{n-1,m} + \sin^2 \frac{\theta_R}{2} \sigma_{33}^{n,m-1} \right)\end{aligned}\quad (20c)$$

$$\dot{\sigma}_{33}^{n,m} = -(2\Gamma_R + \Gamma_L) \sigma_{33}^{n,m} + \Gamma_L \left( \sin^2 \frac{\theta_L}{2} \sigma_{11}^{n,m} + \cos^2 \frac{\theta_L}{2} \sigma_{22}^{n,m} \right) + \frac{\Gamma_L}{2} \sin \theta_L (\sigma_{12}^{n,m} + \sigma_{21}^{n,m}) \quad (20d)$$

$$\begin{aligned}\dot{\sigma}_{12}^{n,m} = & -(i\epsilon + \Gamma_L + \Gamma_R) \sigma_{12}^{n,m} - \frac{\Gamma_L}{2} \sin \theta_L (\sigma_{00}^{n,m} + \sigma_{11}^{n,m} + \sigma_{22}^{n,m} + \sigma_{33}^{n,m}) \\ & + \frac{\Gamma_R}{2} \sin \theta_R (\sigma_{33}^{n-1,m} - \sigma_{33}^{n,m-1})\end{aligned}\quad (20e)$$

Let us trace the origin of each term in these equations taking as an example Eq. (20b), corresponding to  $j = j' = 1$  in Eq.(19). The first, “loss” term in this equation is generated by the transitions  $1 \rightarrow 0 \rightarrow 1$  and  $1 \rightarrow 3 \rightarrow 1$  in Eq. (19). corresponding to the following processes: (a) an electron at the level  $E_1$  (Fig. 3(1)) tunnels to the right reservoir and back to the same state, with the rate  $\Gamma_R$ ; (b) the same electron tunnels to the available continuum states of the left reservoir and back to the level  $E_1$ , with the rate  $\Gamma_L \sin^2(\theta_L/2)$ . This can proceed only via the spin-flip, since the spin-up states in the left reservoir are occupied; (c) an electron from occupied states of the left reservoir tunnels to unoccupied level  $E_2$  of the dot and then back to the same state of the left reservoir, with the rate  $\Gamma_L \sin^2(\theta_L/2)$ .

The second, “gain”, term in Eq. (20b) is generated by the transitions  $0 \rightarrow 1, 0 \rightarrow 1$  and  $3 \rightarrow 1, 3 \rightarrow 1$  of an electron from the left reservoir to the level  $E_1$  and from the level  $E_2$  to

the unoccupied (spin-down) continuum states of the left reservoir.

The third, “loss”, term in Eq. (20b) is generated by the transitions  $2 \rightarrow 0 \rightarrow 1$  and  $2 \rightarrow 3 \rightarrow 1$  via the left reservoir. These transitions involve the following processes: (a) an electron at the level  $E_2$  (Fig. 3(2)) tunnels to an unoccupied, spin-down state of the left reservoir, and then makes the spin-flip transition to the state  $E_1$  of the dot. The rate of this process is  $(1/2)\Gamma_L \sin(\theta_L) \cos(\theta_L/2)$ , as follows from Eq. (19); (b) an electron from one of the occupied states of the left reservoir tunnels to the state  $E_1$  with the corresponding amplitude  $\Omega_L \cos(\theta_L/2)$ . Then an electron on the level  $E_2$  tunnels to the vacant state of the left reservoir with the spin-flip amplitude  $-\Omega_L \sin(\theta_L/2)$ . Since this transition proceeds via two-electron state of the dot, the corresponding permutation prefactor,  $\mathcal{P}_2 = -1$ . As a result, the rate of this (loss) process is  $(1/2)\Gamma_L \sin(\theta_L)$ . Similar transitions via the right reservoir are cancelled. Indeed the electron from the level  $E_2$  can reach the level  $E_1$  by two ways: first through the spin-flip hopping to the right reservoir and then to the level  $E_1$  with no spin-flip, and second, without spin-flip to the right reservoir, and then to the level  $E_1$  with the spin flip. These two amplitudes are of the opposite sign.

The last “gain” term of Eq. (20b) is generated by the transitions  $3 \rightarrow 1, 3 \rightarrow 1$  of an electron from the state in Fig. 3(3) to the spin-up or spin-down states of the right reservoir. The number of electrons in the right reservoir increases by one.

Using these Eqs. (20) we can easily obtain the spin-up and spin-down currents,  $I_{1/2}(t) = \sum_{n,m} n \dot{P}_{n,m}(t)$  and  $I_{-1/2}(t) = \sum_{n,m} m \dot{P}_{n,m}(t)$ , where  $P_{n,m}(t) = \sum_{j=0}^{j=3} \sigma_{jj}^{n,m}$  is a probability of finding  $n$  electrons with spin up and  $m$  electrons with spin down in the right reservoir. One finds

$$I_{1/2}(t) = \Gamma_R \left[ \cos^2 \frac{\theta_R}{2} \sigma_{11}(t) + \sin^2 \frac{\theta_R}{2} \sigma_{22}(t) + \sigma_{33}(t) - \frac{\sin \theta_R}{2} (\sigma_{12}(t) + \sigma_{21}(t)) \right] \quad (21a)$$

$$I_{-1/2}(t) = \Gamma_R \left[ \sin^2 \frac{\theta_R}{2} \sigma_{11}(t) + \cos^2 \frac{\theta_R}{2} \sigma_{22}(t) + \sigma_{33}(t) + \frac{\sin \theta_R}{2} (\sigma_{12}(t) + \sigma_{21}(t)) \right] \quad (21b)$$

where  $\sigma_{jj'}(t) = \sum_{n,m} \sigma_{jj'}^{n,m}(t)$ . (Note that  $\sum_{j=0}^{j=3} \sigma_{jj}(t) = 1$ ). Performing summation over  $n, m$  in Eqs. (20) we obtain the following matrix equation

$$\dot{X}(t) + BX(t) = 0, \quad (22)$$

where  $X(t)$  is a vector  $X = \{\sigma_{00}, \sigma_{11}, \sigma_{22}, \sigma_{33}, \sigma_{12}, \sigma_{21}\}$  and  $B$  is the corresponding  $6 \times 6$  matrix,

$$B = \begin{pmatrix} \Gamma_L & -\Gamma_L \sin^2 \frac{\theta_L}{2} - \Gamma_R & -\Gamma_L \cos^2 \frac{\theta_L}{2} - \Gamma_R & 0 & -\frac{\Gamma_L}{2} \sin \theta_L & -\frac{\Gamma_L}{2} \sin \theta_L \\ -\Gamma_L \cos^2 \frac{\theta_L}{2} & \Gamma_R + 2\Gamma_L \sin^2 \frac{\theta_L}{2} & 0 & -\Gamma_L \cos^2 \frac{\theta_L}{2} - \Gamma_R & \frac{\Gamma_L}{2} \sin \theta_L & \frac{\Gamma_L}{2} \sin \theta_L \\ -\Gamma_L \sin^2 \frac{\theta_L}{2} & 0 & \Gamma_R + 2\Gamma_L \cos^2 \frac{\theta_L}{2} & -\Gamma_L \sin^2 \frac{\theta_L}{2} - \Gamma_R & \frac{\Gamma_L}{2} \sin \theta_L & \frac{\Gamma_L}{2} \sin \theta_L \\ 0 & -\Gamma_L \sin^2 \frac{\theta_L}{2} & -\Gamma_L \cos^2 \frac{\theta_L}{2} & \Gamma_L + 2\Gamma_R & -\frac{\Gamma_L}{2} \sin \theta_L & -\frac{\Gamma_L}{2} \sin \theta_L \\ \frac{\Gamma_L}{2} \sin \theta_L & \frac{\Gamma_L}{2} \sin \theta_L & \frac{\Gamma_L}{2} \sin \theta_L & \frac{\Gamma_L}{2} \sin \theta_L & i\epsilon + \Gamma_t & 0 \\ \frac{\Gamma_L}{2} \sin \theta_L & \frac{\Gamma_L}{2} \sin \theta_L & \frac{\Gamma_L}{2} \sin \theta_L & \frac{\Gamma_L}{2} \sin \theta_L & 0 & -i\epsilon + \Gamma_t \end{pmatrix} \quad (23)$$

Here  $\Gamma_t = \Gamma_L + \Gamma_R$ .

Solving Eqs. (22) and substituting the result into Eqs. (21) we reproduce Eqs. (14),(15) for the polarized current,  $I_{\pm 1/2}(t)$  obtained in the framework of single electron transport. This agreement with the case of non-interacting electrons looks quite remarkable since our rate equations dealing with many-electron states look very different from those obtained in single electron framework. Yet, this is not surprising since in the case of non-interacting electrons the single electron description is valid. In fact, Eqs. (8) can be mapped to Eq. (22) by using  $|\mathbf{b}_i(t)|^2 = \sigma_{ii}(t) + \sigma_{33}(t)$ , where  $i = 1, 2$  and  $\mathbf{b}_1(t)\mathbf{b}_2^*(t) = \sigma_{12}(t)$ .

## B. Noise spectrum of total current for non-interacting electrons

Although the many-body description for non-interacting electrons results in more complicated equations than those using the single electron approach, Eqs. (20) are more appropriate for evaluation of the shot-noise spectrum,  $S(\omega)$ . Let us illustrate this point by evaluating the noise-spectrum of the total current. The latter is a sum of the spin-up and spin-down currents in the final state, whereas the initial current is polarized. For this reason we introduce the density matrix  $\sigma_{jj'}^N(t) = \sum_n \sigma^{n,N-n}(t)$ , obtained from Eqs. (20), where  $N$  denotes

the total number of electrons which have arrived at the right reservoir by time  $t$ . In order to calculate the shot-noise spectrum we use the McDonald formula [4]

$$S(\omega) = 2e^2\omega \int_0^\infty dt \sin(\omega t) \frac{d}{dt} \sum_N N^2 P_N(t) , \quad (24)$$

where  $P_N(t) = \sum_{j=0}^{j=3} \sigma_{jj}^N(t)$ . One easily finds from Eqs. (20) that

$$\sum_N N^2 \dot{P}_N(t) = \Gamma_R \sum_N (2N+1) [\sigma_{11}^N(t) + \sigma_{22}^N(t) + 2\sigma_{33}^N(t)] . \quad (25)$$

Substituting Eq. (25) into the McDonald formula, Eq. (24), we finally obtain

$$S(\omega) = 2e^2\omega\Gamma_R \text{Im} [Z_{11}(\omega) + Z_{22}(\omega) + 2Z_{33}(\omega)] , \quad (26)$$

where  $Z(\omega)$  is a 6-vector,  $Z = \{Z_{00}, Z_{11}, Z_{22}, Z_{33}, Z_{12}Z_{21}\}$ , defined as

$$Z_{ij}(\omega) = \int_0^\infty \sum_N (2N+1) \sigma_{ij}^N(t) \exp(i\omega t) dt . \quad (27)$$

One can find  $Z_{ij}(\omega)$  directly from Eqs. (20) by performing the corresponding summation over  $N$ . As a result one obtains

$$(B - i\omega I)Z(\omega) = \bar{X} + 2\Gamma_R \bar{Y}(\omega) . \quad (28)$$

Here  $B$  is given Eq. (23) and  $I$  is the unit matrix. The 6-vector  $\bar{X}$  corresponds to the stationary solution of Eqs. (22),  $\bar{X} = X(t \rightarrow \infty)$  and  $\bar{Y}(\omega) = \{Y_{11} + Y_{22}, Y_{33}, Y_{33}, 0, 0, 0\}$  where  $Y(\omega) = \{Y_{00}, Y_{11}, Y_{22}, Y_{33}, Y_{33}, Y_{12}, Y_{21}\}$  is given by the equation

$$(B - i\omega I)Y(\omega) = \bar{X} \quad (29)$$

Using Eq. (28) we calculate the ratio of the shot-noise power spectrum to the Schottky noise,  $S(\omega)/2eI$  (Fano factor), where  $I = I(t \rightarrow \infty) = \Gamma_L \Gamma_R / \Gamma_t$ , Eq.(16). In particular, the result has a simple analytical form for a symmetric dot,  $\Gamma_L = \Gamma_R = \Gamma$ . We find

$$\frac{S(\omega)}{2eI} = \frac{2\Gamma^2 + \omega^2}{4\Gamma^2 + \omega^2} + \frac{\Gamma^2 \epsilon^2 \sin^2 \theta_L}{(4\Gamma^2 + \omega^2)(4\Gamma^2 + \omega^2)} . \quad (30)$$

As expected the shot-noise spectrum does not display any peak or dip at frequency corresponding to the Zeeman splitting, since the interference effects are cancelled in the total

current. Yet the noise spectrum depends on the initial polarization of incoming electrons ( $\theta_L$ ), whereas the total current does not (see Eq. (16)). If electrons are initially polarized along the magnetic field inside the dot ( $\hat{\mathbf{n}}$ ), the Fano factor is the same as in the case of resonant tunneling through a single level [14]. With increasing of  $\theta_L$ , however, the current flows through two levels of the Zeeman doublet. This leads to an additional contribution to the shot noise, described by the second term of Eq. (30).

### C. Ferromagnetic reservoirs.

Let us consider ferromagnetic reservoirs polarized along  $\mathbf{n}$  and  $\mathbf{n}'$  directions, Fig. 1. In this case the rate equations (20) have to be modified since there are no available spin-down states in the left and right reservoirs. One easily obtains the following rate equations for the density matrix  $\sigma_{jj'}^n(t)$ , where  $n$  denotes the number of electron, arriving at the collector by time  $t$ :

$$\dot{\sigma}_{00}^n = -\Gamma_L \sigma_{00}^n + \Gamma_R \cos^2 \frac{\theta_R}{2} \sigma_{11}^{n-1} + \Gamma_R \sin^2 \frac{\theta_R}{2} \sigma_{22}^{n-1} - \frac{\Gamma_R}{2} \sin \theta_R (\sigma_{12}^{n-1} + \sigma_{21}^{n-1}) \quad (31a)$$

$$\begin{aligned} \dot{\sigma}_{11}^n = & - \left( \Gamma_L \sin^2 \frac{\theta_L}{2} + \Gamma_R \cos^2 \frac{\theta_R}{2} \right) \sigma_{11}^n + \Gamma_L \cos^2 \frac{\theta_L}{2} \sigma_{00}^n \\ & - \frac{1}{4} (\Gamma_L \sin \theta_L - \Gamma_R \sin \theta_R) (\sigma_{12}^n + \sigma_{21}^n) + \Gamma_R \sin^2 \frac{\theta_R}{2} \sigma_{33}^{n-1} \end{aligned} \quad (31b)$$

$$\begin{aligned} \dot{\sigma}_{22}^n = & - \left( \Gamma_L \cos^2 \frac{\theta_L}{2} + \Gamma_R \sin^2 \frac{\theta_R}{2} \right) \sigma_{22}^n + \Gamma_L \sin^2 \frac{\theta_L}{2} \sigma_{00}^n \\ & - \frac{1}{4} (\Gamma_L \sin \theta_L - \Gamma_R \sin \theta_R) (\sigma_{12}^n + \sigma_{21}^n) + \Gamma_R \cos^2 \frac{\theta_R}{2} \sigma_{33}^{n-1} \end{aligned} \quad (31c)$$

$$\dot{\sigma}_{33}^n = -\Gamma_R \sigma_{33}^n + \Gamma_L \left( \sin^2 \frac{\theta_L}{2} \sigma_{11}^n + \cos^2 \frac{\theta_L}{2} \sigma_{22}^n \right) + \frac{\Gamma_L}{2} \sin \theta_L (\sigma_{12}^n + \sigma_{21}^n) \quad (31d)$$

$$\begin{aligned} \dot{\sigma}_{12}^n = & - \left( i\epsilon + \frac{\Gamma_L + \Gamma_R}{2} \right) \sigma_{12}^n - \frac{\Gamma_L}{2} \sin \theta_L \sigma_{00}^n - \frac{\Gamma_L - \Gamma_R}{4} \sin \theta_L (\sigma_{11}^n + \sigma_{22}^n) \\ & + \frac{\Gamma_R}{2} \sin \theta_R \sigma_{33}^{n-1} \end{aligned} \quad (31e)$$

Using these equations we first evaluate the average current,  $I(t) \equiv I_{1/2}(t)$  given by Eq. (21a) with  $\sigma_{jj'}(t) = \sum_n \sigma_{jj'}^n(t)$ . The latter quantities are obtained from a summation of



Eqs. (31) over  $n$ . As a result Eqs. (31) are reduced to the matrix equation (22), where  $B$  is the corresponding  $6 \times 6$  matrix of the coefficients of Eqs. (31). Solving this equation we find the average current  $I(t)$ . For instance, in the case of  $\theta_L = \theta_R$  one finds for the stationary current,  $I = I(\infty) = \Gamma_L \Gamma_R / (\Gamma_L + \Gamma_R)$ . The same expression one obtains for the resonant tunneling of unpolarized electrons through a single level.

The time dependence of the average current,  $I(t)$ , is displayed in Fig. 4 for symmetric and asymmetric dots,  $\Gamma_L = \Gamma_R = 0.1\epsilon$  and  $\Gamma_L = \epsilon$ ,  $\Gamma_R = 0.1\epsilon$ , respectively. Comparing with Fig. 2 one finds that the oscillations in the average current are more pronounced in the case of ferromagnetic reservoirs. This can be anticipated since the corresponding spin-flip transitions via the spin-down states of the reservoirs do not exist. We remind that precisely these transitions resulted in the cancelation of the interference effects in the previous case

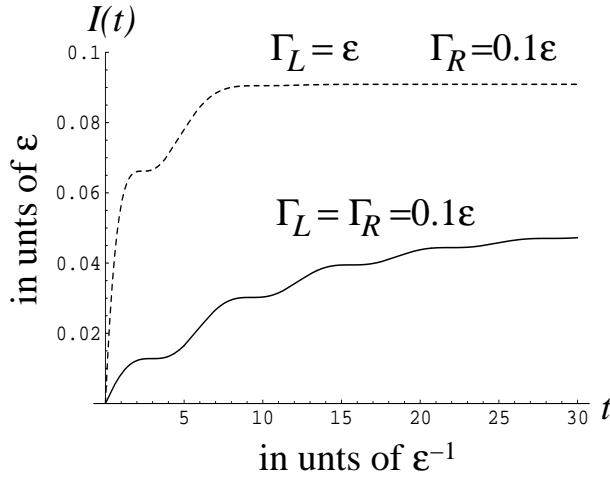


Fig. 4. Polarized resonant current through the Zeeman doublet in the case of ferromagnetic reservoirs for  $\theta_L = \theta_R = \pi/2$ . Solid line corresponds to  $\Gamma_L = \Gamma_R = 0.1\epsilon$  and dashed line to  $\Gamma_L = \epsilon$  and  $\Gamma_R = 0.1\epsilon$ .

Now we can evaluate the shot-noise spectrum,  $S(\omega)$  by using the McDonald formula. One obtains from Eqs. (24) and (31)

$$S(\omega) = 2e^2 \omega \Gamma_R \text{Im} \left\{ \cos^2 \frac{\theta_R}{2} Z_{11}(\omega) + \sin^2 \frac{\theta_R}{2} Z_{22}(\omega) + Z_{33}(\omega) \right\}$$

$$- \frac{\sin \theta_R}{2} [Z_{12}(\omega) + Z_{21}(\omega)] \Big\} , \quad (32)$$

where  $Z(\omega)$  is given by Eq. (28) with the matrix  $B$  corresponding to Eqs. (31) and  $\bar{Y} = \{\bar{Y}_{00}, \bar{Y}_{11}, \bar{Y}_{22}, 0, \bar{Y}_{12}, \bar{Y}_{21}\}$ . Here  $\bar{Y}_{00} = \cos^2 \frac{\theta_R}{2} Y_{11} + \sin^2 \frac{\theta_R}{2} Y_{22} - \frac{\sin \theta_R}{2} (Y_{12} + Y_{21})$ ,  $\bar{Y}_{11} = \sin^2 \frac{\theta_R}{2} Y_{33}$ ,  $\bar{Y}_{22} = \cos^2 \frac{\theta_R}{2} Y_{33}$ , and  $\bar{Y}_{12} = \bar{Y}_{21} = \frac{\sin \theta_R}{2} Y_{33}$ , while  $Y_{jj'} = Y_{jj'}(\omega)$  are given by Eq. (29).

The corresponding Fano factor is shown in Fig. 5 for the same parameters as in Fig. 4. It clearly displays a dip at Zeeman frequency for a symmetric dot. It reflects damped oscillations in the average current, shown in Fig. 4. The dip, however, almost disappears for an asymmetric dot with large  $\Gamma_L$ .

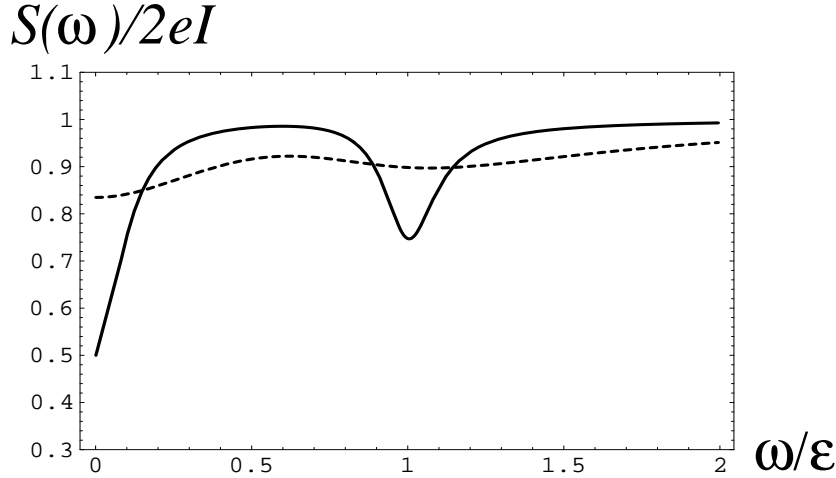


Fig. 5. Fano factor versus  $\omega$  for polarized electron current in the case of ferromagnetic reservoirs for  $\theta_L, \theta_R = \pi/2$  Solid line corresponds to  $\Gamma_L = \Gamma_R = 0.1\epsilon$  and dashed line to  $\Gamma_L = \epsilon$  and  $\Gamma_R = 0.1\epsilon$ .

#### IV. COULOMB BLOCKADE

Let us introduce strong Coulomb repulsion inside the dot,  $U_C \gg \mu_L - E_1$ , so that the state (3) in Fig. 3 is not available. As a result the corresponding rate equations have even

a simpler form than those found for non-interacting electrons. Consider again the case of ferromagnetic reservoirs, where the quantum interference effects are mostly pronounced. The corresponding rate equations for the case of Coulomb blockade can be obtained from Eqs. (31) for non-interacting electrons, by eliminating configurations with two electrons in the dot. In the following we consider separately the electron current in the right and in the left reservoirs.

### A. Collector current.

The electrical current in the right reservoir and its power spectrum are obtained from the following rate equation

$$\dot{\sigma}_{00}^n = -\Gamma_L \sigma_{00}^n + \Gamma_R \cos^2 \frac{\theta_R}{2} \sigma_{11}^{n-1} + \Gamma_R \sin^2 \frac{\theta_R}{2} \sigma_{22}^{n-1} - \frac{\Gamma_R}{2} \sin \theta_R (\sigma_{12}^{n-1} + \sigma_{21}^{n-1}) \quad (33a)$$

$$\dot{\sigma}_{11}^n = -\Gamma_R \cos^2 \frac{\theta_R}{2} \sigma_{11}^n + \Gamma_L \cos^2 \frac{\theta_L}{2} \sigma_{00}^n + \frac{\Gamma_R}{4} \sin \theta_R (\sigma_{12}^n + \sigma_{21}^n) \quad (33b)$$

$$\dot{\sigma}_{22}^n = -\Gamma_R \sin^2 \frac{\theta_R}{2} \sigma_{22}^n + \Gamma_L \sin^2 \frac{\theta_L}{2} \sigma_{00}^n + \frac{\Gamma_R}{4} \sin \theta_R (\sigma_{12}^n + \sigma_{21}^n) \quad (33c)$$

$$\dot{\sigma}_{12}^n = -\left(i\epsilon + \frac{\Gamma_R}{2}\right) \sigma_{12}^n - \frac{\Gamma_L}{2} \sin \theta_L \sigma_{00}^n + \frac{\Gamma_R}{4} \sin \theta_R (\sigma_{11}^n + \sigma_{22}^n) \quad (33d)$$

Using these equations one finds for the average (polarized) current in the collector

$$I_R(t) = \Gamma_R \left[ \cos^2 \frac{\theta_R}{2} \sigma_{11}(t) + \sin^2 \frac{\theta_R}{2} \sigma_{22}(t) - \frac{\sin \theta_R}{2} (\sigma_{12}(t) + \sigma_{21}(t)) \right] \quad (34)$$

where  $\sigma_{jj'}(t) = \sum_{n,m} \sigma_{jj'}^{n,m}(t)$  are obtained from Eq. (22) for  $X = \{\sigma_{00}, \sigma_{11}, \sigma_{22}, \sigma_{12}, \sigma_{21}\}$ , and the matrix  $B$  is given by

$$B = \begin{pmatrix} \Gamma_L & -\Gamma_R \cos^2 \frac{\theta_R}{2} & -\Gamma_R \sin^2 \frac{\theta_R}{2} & \frac{\Gamma_R}{2} \sin \theta_R & \frac{\Gamma_R}{2} \sin \theta_R \\ -\Gamma_L \cos^2 \frac{\theta_L}{2} & \Gamma_R \cos^2 \frac{\theta_R}{2} & 0 & -\frac{\Gamma_R}{4} \sin \theta_R & -\frac{\Gamma_R}{4} \sin \theta_R \\ -\Gamma_L \sin^2 \frac{\theta_L}{2} & 0 & \Gamma_R \sin^2 \frac{\theta_R}{2} & -\frac{\Gamma_R}{4} \sin \theta_R & -\frac{\Gamma_R}{4} \sin \theta_R \\ \frac{\Gamma_L}{2} \sin \theta_L & -\frac{\Gamma_R}{4} \sin \theta_R & -\frac{\Gamma_R}{4} \sin \theta_R & i\epsilon + \frac{\Gamma_R}{2} & 0 \\ \frac{\Gamma_L}{2} \sin \theta_L & -\frac{\Gamma_R}{4} \sin \theta_R & -\frac{\Gamma_R}{4} \sin \theta_R & 0 & -i\epsilon + \frac{\Gamma_R}{2} \end{pmatrix} \quad (35)$$

Solving such a modified Eq. (22) for the case of  $\theta_L = \theta_R$  one finds for the stationary current,

$$I_R = I_R(\infty) = \frac{\Gamma_L \Gamma_R}{2\Gamma_L + \Gamma_R} \quad (36)$$

This expression shows an asymmetry with respect to the widths  $\Gamma_L$  and  $\Gamma_R$ , in contrast with the non-interacting case. The reason is that an electron enters the dot from the left reservoir with the rate  $2\Gamma_L$ . However, it leaves it with the rate  $\Gamma_R$ , since the state with two levels of the dot occupied is forbidden.

Respectively, the shot-noise power spectrum for the collector current is given by

$$S_R(\omega) = 2e^2\omega\Gamma_R \text{Im} \left\{ \cos^2 \frac{\theta_R}{2} Z_{11}(\omega) + \sin^2 \frac{\theta_R}{2} Z_{22}(\omega) - \frac{\sin \theta_R}{2} [Z_{12}(\omega) + Z_{21}(\omega)] \right\}. \quad (37)$$

Here  $Z_{ij}(\omega)$  are obtained from Eqs. (28),(29), where  $\bar{Y} = \{\bar{Y}_{00}, 0, 0, 0, 0\}$  and  $\bar{Y}_{00} = \cos^2 \frac{\theta_R}{2} Y_{11} + \sin^2 \frac{\theta_R}{2} Y_{22} - \frac{\sin \theta_R}{2} (Y_{12} + Y_{21})$ .

The results of our calculations of  $S(\omega)$  for symmetric and asymmetric quantum dots in the case of Coulomb blockade are shown in Fig. 6.

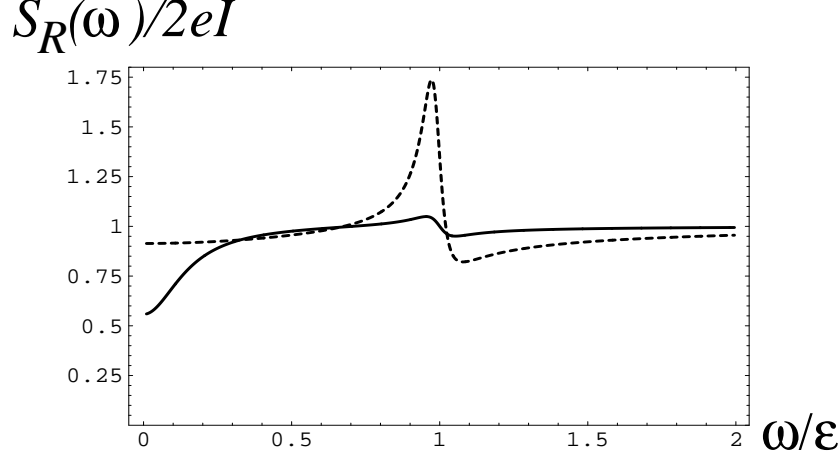


Fig. 6. Fano factor versus  $\omega$  for polarized collector current in the case of ferromagnetic reservoirs and Coulomb blockade for  $\theta_L, \theta_R = \pi/2$  Solid line corresponds to  $\Gamma_L = \Gamma_R = 0.1\epsilon$  and dashed line to  $\Gamma_L = \epsilon$  and  $\Gamma_R = 0.1\epsilon$ .

## B. Emitter current.

Let us consider the electric current and its power spectrum in the left reservoir. These quantities are determined from the density-matrix  $\sigma_{jj'}^p$ , where  $p$  is the number of electrons that left the emitter by time  $t$  (the number of holes in the left reservoir). The corresponding rate equations are similar to Eqs. (33). One finds

$$\dot{\sigma}_{00}^p = -\Gamma_L \sigma_{00}^p + \Gamma_R \cos^2 \frac{\theta_R}{2} \sigma_{11}^p + \Gamma_R \sin^2 \frac{\theta_R}{2} \sigma_{22}^p - \frac{\Gamma_R}{2} \sin \theta_R (\sigma_{12}^p + \sigma_{21}^p) \quad (38a)$$

$$\dot{\sigma}_{11}^p = -\Gamma_R \cos^2 \frac{\theta_R}{2} \sigma_{11}^p + \Gamma_L \cos^2 \frac{\theta_L}{2} \sigma_{00}^{p-1} + \frac{\Gamma_R}{4} \sin \theta_R (\sigma_{12}^p + \sigma_{21}^p) \quad (38b)$$

$$\dot{\sigma}_{22}^p = -\Gamma_R \sin^2 \frac{\theta_R}{2} \sigma_{22}^p + \Gamma_L \sin^2 \frac{\theta_L}{2} \sigma_{00}^{p-1} + \frac{\Gamma_R}{4} \sin \theta_R (\sigma_{12}^p + \sigma_{21}^p) \quad (38c)$$

$$\dot{\sigma}_{12}^p = -\left(i\epsilon + \frac{\Gamma_R}{2}\right) \sigma_{12}^p - \frac{\Gamma_L}{2} \sin \theta_L \sigma_{00}^{p-1} + \frac{\Gamma_R}{4} \sin \theta_R (\sigma_{11}^p + \sigma_{22}^p) \quad (38d)$$

The average emitter current in the left reservoir is given by  $I_L(t) = \Gamma_L \sigma_{00}(t)$ , which differs from Eq. (34) describing the collector current,  $I_R(t)$ . Yet, as expected, their stationary values coincide,  $I_L(\infty) = I_R(\infty)$ , Eq. (36).

The shot-noise power spectrum of the emitter current is given

$$S_L(\omega) = 2e^2 \omega \Gamma_L \sigma_{00}(\omega) \quad (39)$$

instead of Eq. (37) for  $S_R(\omega)$ , where  $Z_{ij}(\omega)$  are obtained from Eqs. (28),(29). Yet,  $\bar{Y}(\omega) = \{0, \cos^2 \frac{\theta_L}{2}, \sin^2 \frac{\theta_L}{2}, -\frac{\sin \theta_L}{2}, -\frac{\sin \theta_L}{2}\} Y_{00}(\omega)$ , in contrast with the corresponding expression for  $S_R(\omega)$ . Nevertheless, despite expressions for  $S_{L,R}(\omega)$  are quite different, one finds that the shot-noise power of the emitter current is the same as that in the collector current,  $S_L(\omega) = S_R(\omega)$ .

## C. Circuit current.

In general the circuit current is given by  $I_c(t) = \alpha I_L(t) + \beta I_R(t)$ , where the coefficients  $\alpha, \beta$  with  $\alpha + \beta = 1$  depend on each junction capacities [15]. Using charge conservation,  $I_L = I_R + \dot{Q}$ , where  $Q$  is charge in the dot, one finds

$$I_c(t)I_c(0) = \alpha I_L(t)I_L(0) + \beta I_R(t)I_R(0) - \alpha\beta\dot{Q}(t)\dot{Q}(0). \quad (40)$$

Using this relation one finds a simple expression for the noise spectrum of the circuit current [4,16]

$$S_c(\omega) = \alpha S_L(\omega) + \beta S_R(\omega) - \alpha\beta\omega^2 S_Q(\omega). \quad (41)$$

where  $S_Q(\omega)$  is Fourier transform of the charge correlator. This quantity can be obtained straightforwardly from the matrix equation (29), where  $B$  is given by Eq. (35) and the  $\bar{X}$  is replaced by the 5-vector  $\{0, \sigma_{11}(\infty), \sigma_{22}(\infty), 0, 0\}$ . Then  $S_Q(\omega) = 4\text{Re}[Y_{11}(\omega) + Y_{22}(\omega)]$ .

The results of our calculations of  $S_c(\omega)$  for  $\alpha = \beta = 1/2$  are shown in Fig. 7.

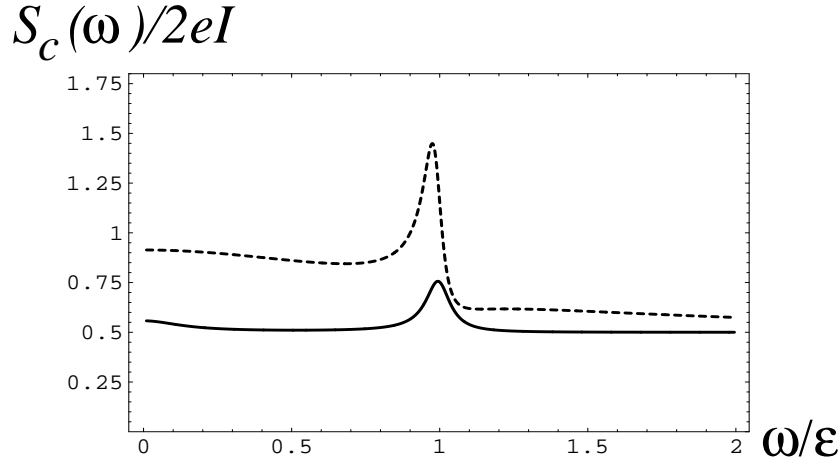


Fig. 7. Fano factor for the circuit ( $\alpha = \beta = 1/2$  versus  $\omega$  for polarized electron current in the case of ferromagnetic reservoirs and Coulomb blockade for  $\theta_L, \theta_R = \pi/2$ . Solid line corresponds to  $\Gamma_L = \Gamma_R = 0.1\epsilon$  and dashed line to  $\Gamma_L = \epsilon$  and  $\Gamma_R = 0.1\epsilon$ .

One finds from Figs. 6 and 7 that the Coulomb blockade modifies the current spectrum very drastically with respect to the non-interacting case, Fig. 5.

## V. CONCLUSIONS

In this paper, we study the interference effects in magneto-transport through Zeeman split levels of quantum dots or impurities. We concentrated on the time-dependent properties and power spectrum of the electric current by applying a new approach of quantum rate equations, which is mostly suitable for this type of problems. We explicitly demonstrated that our method produces the same results as a single electron approach, widely used for a description of non-interacting electron transport. Yet the quantum rate equations method is valid also in the case of interacting electrons by accounting the Coulomb blockade in the most simple and precise way.

Our results indicate that the Coulomb blockade plays an important role in the spectral properties of the transport current. First of all, in the presence of Coulomb blockade the signal-to-noise ratio significantly amplifies, as one can observe from the results in the previous sections. Probably this is a consequence of a prohibition of double occupation of the resonant level in the quantum dot. Indeed, when two electrons in the dot are present, the interference effects are suppressed due to the “randomization” of the relative phase. Interestingly, the dip in the noise spectrum for the noninteracting electrons is replaced by a peak as result of Coulomb interaction. Clearly interaction modifies the phase of the electrons tunneling through the dot, which “flips” the spectral feature in the noise. The details of such a very interesting phenomena must be studied in the future.

We emphasize that the coherent oscillations in the current can be observed only for polarized current and disappear in the unpolarized current. This is different from the resonant transport through two orbital levels of a quantum dot or impurity, where the quantum interference effects can be observed even in unpolarized case. Therefore it is most naturally to use ferromagnetic leads for observation and utilization of quantum interference effect in the magneto-transport. Thus our calculations were mostly concentrated on this case. Our results show explicitly an appearance of peak or dip at the frequency near the Zeemann splitting (Larmour frequency). We believe that this phenomenon can be used for noise spectroscopy

of quantum dots or impurities. Indeed, the Zeeman splitting of a localized quantum dot orbital must be sensitive to local magnetic fields, and therefore one can hope that such coherent effect, if observed experimentally, may allow for detection of local hyperfine structure of the dot/impurity. This, however, must be a subject of a separate investigation.

## **VI. ACKNOWLEDGEMENT**

We thank J. Brown, L. Fedichkin, M. B. Hastings, M. Hawley, and I. Martin for valuable discussions. The was was supported by US DOE. D. M. was supported, in part, by the US NSF grant DMR-0121146.



## REFERENCES

- [1] S.A. Gurvitz, IEEE Transactions on Nanotechnology **4**, 45 (2005); (cond-mat/0406010).
- [2] Y. Manassen *et al.*, Phys. Rev. Lett. **62**, 2531 (1989); D. Shachal, Y. Manassen, Phys. Rev. B **46**, 4795 (1992); Y. Manassen *et al.*, Phys. Rev. B **61**, 16223 (2000).
- [3] C. Durkan, and M. E. Welland, Appl. Phys. Lett. **80**, 458 (2002).
- [4] D. Mozyrsky, L. Fedichkin, S.A. Gurvitz and G.P. Berman, Phys. Rev. B **66**, 161313 (2002).
- [5] M. Braun, J.König and J. Martinek, Phys. Rev. B **70**, 195345 (2004); *ibid*, Superlattices and Microstructures **37**, 333 (2005).
- [6] S. Braig and P. W. Brouwer, Phys. Rev. B **71**, 195324 (2005).
- [7] L. Y. Gorelik, S. I. Kulinich, R. I. Shekhter, M. Jonson, and V. M. Vinokur, cond-mat/0502243 (unpublished).
- [8] S. Yuasa, T. Nagahama, A. Fukushima, Y. Suzuki, and K. Ando, Nature Materials **3**, 868 (2004).
- [9] S.A. Gurvitz and Ya.S. Prager, Phys. Rev. B **53**, 15932 (1996).
- [10] S.A. Gurvitz, Phys. Rev. B **57**, 6602 (1998).
- [11] J. Bardeen, Phys. Rev. Lett. **6** 57, (1961); S.A. Gurvitz, “Two-potential approach to multi-dimensional tunneling”, in *Michael Marinov Memorial Volume, Multiple facets of quantization and supersymmetry*, (Eds. M. Olshanetsky and A. Vainshtein, World Scientific), p. 91, (2002), (nucl-th/0111076).
- [12] I. Bar-Joseph and S.A. Gurvitz, Phys. Rev. B **44**, 3332 (1991); S.A. Gurvitz, Phys. Rev. B **44**, 11924 (1991).
- [13] Note that in the large bias limit considered here, the off-diagonal matrix elements in the

reservoir variables,  $\sigma_{jj'}^{nn',mm'}$ , are decoupled in the equation of motion from the diagonal elements,  $\sigma_{jj'}^{nn,mm} \equiv \sigma_{jj'}^{n,m}$  (see also S.A. Gurvitz, Quantum Information Processing, **2**, 15 (2003)).

- [14] L.Y. Chen and C.S. Ting, Phys. Rev. B **43**, 4534 (1991); *ibid*, **46**, 4714 (1992); B. Elattari and S.A. Gurvitz, Phys. Lett. A **292**, 289 (2003).
- [15] Y.M. Blanter and M. Büttiker, Phys. Rep. **36**, 1 (2000).
- [16] R. Aguado and T. Brandes, Phys. Rev. Lett. **92**, 206601 (2004).